Iranian Journal of Analytical Chemistry
Volume 11, Issue 2, September 2024 (133-142) Original Research Article

مجله ایرانی شیمی تجزیه
دوره ۱۱، شماره ۲، مهرماه (۱۴۲-۱۳۳)

Investigation of the Effect of Polyaniline Content on the Catalytic Activity of Fe_3O_4/GO Nanocomposite

Robab Mohammadi
Department of Chemistry, Payame Noor University, P.O. box 19395-3697, Tehran, Iran

Received: 7 June 2024 **Accepted:** 4 September 2024
DOI: 10.30473/IJAC.2024.72388.1307

Abstract
In this research, Fe_3O_4, Fe_3O_4/graphene oxide (Fe_3O_4/GO) and polyaniline-Fe_3O_4/GO with various content of polyaniline were prepared and characterized by different analysis methods such as XRD, SEM, EDX, and FT-IR. The prepared samples were used to remove methyl red as an anionic dye from aqueous solutions. Polyaniline-Fe_3O_4/GO nanocomposite showed high catalytic activity, which is partly because of the sensitizing influence of polyaniline and the low recombination rate due to the graphene oxide electron scavenging property. The photodegradation reaction fit well to a Langmuir-Hinshelwood kinetic model implying the reaction rate is depended on initial adsorption step. Also, in polyaniline-Fe_3O_4/GO samples, the polyaniline content can play a significant role in affecting photocatalytic activity of photocatalysts. Based on results, when the content of polyaniline is more increased above its optimum value, the photocatalytic performance decreased. Furthermore, the efficiency of polyaniline-Fe_3O_4/GO nanocomposite was investigated to compare between adsorption and photodegradation of methyl red from aqueous solution. Based on results, the removal rate of methyl red via polyaniline-Fe_3O_4/GO nanocomposite under photocatalytic process was considerably higher than the adsorption process. To understand the nature of adsorption procedure, the equilibrium adsorption isotherms were investigated. The linear correlation coefficients of Langmuir and Freundlich isotherms were obtained. Based on results, Langmuir isotherm model fitted the experimental data better than Freundlich isotherm model. According to the Langmuir isotherm model, the maximum adsorption capacity of polyaniline-Fe_3O_4/GO nanocomposite for sequestering methyl red was about 101.72 mg g^{-1}.

Keywords
Polyaniline- Fe_3O_4/GO; Methyl Red; Photocatalytic Activity; Adsorption Process.

1. INTRODUCTION

With the progression of global industrialization, environmental pollution becomes a more serious issue and, thus, has received considerable attention [1]. The amount of suitable water for drinking, agriculture, and farming, has decreased through the years making this an important issue for waste water treatment and reduction. Synthetic dyes are applied extensively in many industries such as: paper generation, leather tanning, food technology, photoelectrochemical cells, and hair colorings. Synthetic dyes are a significant contributor to water pollution and have been proved to be harmful to humans [2].

In past decades, advanced oxidation processes (AOPs) such as Fenton, photo-Fenton, ozonation, and wet air oxidation have been applied successfully for the removal of dyes into environmentally friendly products. AOPs are based on the production of reactive hydroxyl radical in the aqueous solution for the oxidation and mineralization of dyes into CO_2 and water [3]. In particular, iron (Fe)-based heterogeneous catalyst materials (e.g., Fe_3O_4) are regarded as promising candidates for AOPs process because of their high natural abundance, low price, and they could easily prevent secondary pollution through their recovery performance. However, Fe_3O_4 nanoparticles may aggregate in the solution, which can decrease their surface area and cause lower stability and catalytic efficiency [4]. Thus, it is necessary to apply a proper support that can enhance their overall performance. Studies of graphene either as a catalytic support or as a metal-free catalyst, have been summarized in some comprehensive reviews [2]. Graphene is a two-dimensional sheet material with atomic thickness composed of the honeycomb rings produced via sp2-bonded carbon atoms. The large theoretical specific surface area of graphene (about 2630 m^2 g^{-1}) and the abundant functional groups of graphene oxide (GO) make them potential to be applied for degradation of organic dyes. So, graphene because of its high conductivity and mobility can act as an electron scavenger which can decline the recombination rate [5]. Therefore, it is believed that a nanocomposite of Fe_3O_4/GO will exhibit enhanced photocatalytic activity because of the low band gap, low recombination rate and high absorption under ultraviolet (UV)

* Corresponding author:
R. Mohammadi; E-mail: mohammadi_rb@yahoo.com, r.mohammadi@pnu.ac.ir

and visible region, due to the synergism between the constituents. Based on researches, the key problem to exfoliate the graphite layers is to overcome or destroy the strong Vander Waals forces between the layers. It is known that the intercalation of metal cations and ring compounds containing π-electron can effectively exfoliate graphite as graphene. Polyaniline is a nitrogen-containing conductive polymer. Because of the π-electron conjugation structure, polyaniline can well exfoliate the graphite as graphene sheets via the intercalation polymerization of the protonated aniline. What's more, polyaniline is helpful to increase the adsorption property of magnetic graphene-based adsorbents because of the introduction of large contents of amine and imine groups. The aim of the present work is to prepare Fe_3O_4, Fe_3O_4/GO and polyaniline-Fe_3O_4/GO nanomaterials and investigate the photocatalytic activity and adsorption capacity of prepared samples for the removal of an anionic dye (methyl red) from aqueous solutions. Polyaniline value may play an important role in affecting catalytic activity of polyaniline-Fe_3O_4/GO nanocomposite. Therefore, the effect of polyaniline content in the removal of methyl red as a pollutant model was evaluated. To the best of our knowledge, there is no report on the investigation of the effect of polyaniline value for the removal of dyes using polyaniline-Fe_3O_4/GO nanocomposite.

2. EXPERIMENTAL

2.1. Materials and Methods

Iron (III) chloride hexahydrate ($FeCl_3 \cdot 6H_2O$), Iron (II) chloride tetrahydrate ($FeCl_2 \cdot 4H_2O$), ammonium hydroxide (28% v/v, $NH_3 \cdot H_2O$), graphite powder (purity 99.999%), sodium hydroxide, nitric acid, sulfuric acid, potassium chlorate, hydrochloric acid, aniline, ammonium persulphate (APS) and methyl red were purchased from Merck Co. (Germany). All chemicals were used as received except aniline which was distilled under reduced pressure and kept below 4°C before used for synthesis. Deionized water was used in all synthesis.

2.1.1. Preparation of Fe_3O_4 nanoparticles

Fe_3O_4 nanoparticles were synthesized by reverse co precipitation method using ammonia as precipitation agent. In short, 5 mL of 1 mol L^{-1} $FeCl_3.6H_2O$ and 10 mL of 0.5 mol L^{-1} $FeCl_2.4H_2O$ solutions were mixed. The mixture was added drop wise into 20 mL of 3.5 mol L^{-1} ammonium hydroxide solution at 60°C under ultrasound irradiation. The reaction proceeded for 30 min upon completion of the reaction, the resulting black iron oxide nanoparticles were collected with the help of a strong magnet and washed several times with deionized water.

2.1.2. Preparation of GO

Graphene was synthesized via Staudenmaier method. Briefly, 5 g graphite was reacted with 45 mL concentrated nitric acid and 90 mL sulfuric acid and 55 g potassium chlorate. To inhibit any sudden enhancement in temperature, the potassium chlorate was gradually added under constant stirring for 30 min and mixture was stirred for 72 h at room temperature. The mixture was added to water after completing the reaction, washed with a 5% solution of HCl, and deionized water repeatedly until the pH of the filtrate was neutral. The dried graphene was placed in a quartz boat and inserted into a tubular furnace preheated to 1050 °C and kept at this temperature for 30 s.

2.1.3. Preparation of Fe_3O_4/GO materials

Fe_3O_4/Graphene oxide materials were synthesized via co-precipitating pre-hydrolyzed ferric and ferrous salts in the presence of Graphene. An aqueous solution (100 mL) containing $FeCl_3 \cdot 6H_2O$ (4 mmol) and ($FeCl_2 \cdot 4H_2O$ (2 mmol)) was synthesized with an initial pH of 1.48 and subsequently adjusted to pH 4 by addition of NaOH (1 M). 5 mg of Graphene was dissolved in a solution of 90 mL distilled water and 30 mL ethanol by ultrasonic treatment for 2 h and gradually added into the iron oxide solution under constant stirring for 30 min. The pH was adjusted to 10 via adding NaOH (1 M) to the mixture which was then aged at constant stirring for a further 40 min at room temperature. The resulting black precipitate was magnetically separated and washed three times with deionized water and ethanol followed by drying for 48 h in an oven at 70°C. The synthesized sample was designated as Fe_3O_4/Graphene oxide.

2.1.4. Preparation of polyaniline-Fe_3O_4/GO composite material

Polyaniline-Fe_3O_4/GO nanocomposites with various polyaniline contents were prepared via chemical oxidative polymerization of aniline in the presence of Fe_3O_4/GO particles. First, 1 g of nanocrystalline Fe_3O_4/GO particles were dispersed into 150 mL of 1 mol L^{-1} HCl aqueous solution with ultrasonic vibrations for 10 min to obtain a homogeneous suspension. Quantitative aniline was added into this mixture dropwise under vigorously stirring in the ice-water bath, after which APS was dissolved in 1 mol L^{-1} HCl aqueous solution with the molar ratio of aniline to APS (1:0.25) was added to the reaction vessel. Then, the mixture was allowed to polymerize under stirring for 2 h. Finally, polyaniline-Fe_3O_4/GO nanocomposites were filtered and washed several times with distilled water and ethanol and kept in a vacuum oven at 60°C for 24 h till the constant mass was

DOI: 10.30473/IJAC.2024.72388.1307

reached. In the experiment, various initial weight ratios of aniline to Fe_3O_4/GO (4%, 8%, 12%, 16% and 20%) were used to obtain the optimum content of aniline. The prepared samples were designated as 4 polyaniline-Fe_3O_4/GO, 8 polyaniline-Fe_3O_4/GO, 12 polyaniline-Fe_3O_4/GO, 16 polyaniline-Fe_3O_4/GO and 20 polyaniline-Fe_3O_4/GO respectively. Finally, the best catalyst procured in this method was designated as polyaniline-Fe_3O_4/GO.

2.2. Characterization

The crystal structure of prepared samples was recorded by X-ray diffraction (XRD) (Siemens/D5000) with Cu Kα radiation (0.15478 nm) in the 2θ scan range of 10°–70°. The morphology and texture of prepared samples were measured via scanning electron microscope (SEM, LEO 440i, Leo Electron Microscopy, Cambridge, England). The chemical composition of the synthesized nanocomposite was analyzed by an energy-dispersive X-ray spectroscopy (EDX) system. Fourier transform infrared spectroscopy (FTIR) analysis of samples was performed on a Nicolet 560 FTIR spectrometer. The samples were prepared by mixing with KBr and pressing into a compact pellet.

2.3. Studies and analysis

Removal of methyl red under black light irradiation was applied as a model reaction to evaluate the catalytic activity of synthesized samples. Photocatalytic activity measurements were carried out at atmospheric pressure in a batch quartz reactor. The photocatalytic removal of methyl red was measured at ambient pressure and room temperature in a batch quartz reactor, as previously reported [6]. Artificial irradiation was provided by 36 W (UV-A) mercury lamp (Philips, Holland) with a wavelength peak at 365 nm positioned above the photoreactor. In each run, 40 mg of synthesized catalyst and desired amount of methyl red were fed into the quartz tube reactor and allowed to establish an adsorption–desorption equilibrium for 25 min in the darkness. The zero-time reading was obtained from blank solution kept in the dark. While vigorous stirring, the reaction mixture was irradiated via black light. The residual of methyl red was detected using UV-vis Perkin-Elmer 550 SE spectrophotometer at wavelength of 520 nm. Experimental setup for the adsorption of methyl red by polyaniline-Fe_3O_4/GO nanocomposite was similar to that of the photocatalytic degradation of methyl red. However, for the batch adsorptive degradation of methyl red by polyaniline- Fe_3O_4/GO nanocomposite without light irradiation, the setup was placed inside a fully covered box in order to inhibit any exposure toward light irradiation.

3. RESULTS AND DISCUSSION

3.1. Characterization of prepared nanocomposite

3.1.1 X-ray diffraction (XRD)

XRD pattern of polyaniline-Fe_3O_4/GO nanocomposite is shown in Fig. 1. The peaks at 2θ values of 30.8, 36.4, 43.9, 54.5, 58.1 and 63.9 are indexed as the diffractions of (220), (311), (400), (422), (511) and (440) respectively, which resembles the standard diffraction spectrum of Fe_3O_4 (JCPDS card No: 19-0629) with respect to its reflection peaks positions [7]. The sharpness of the peaks clearly indicates that the prepared sample had a highly crystalline nature. These crystalline entities show the typical pattern of Fe_3O_4, and there was no other phase such as Fe_2O_3 or $Fe(OH)_3$, which were the usual co-products in chemical reverse coprecipitation procedure. In explanation, when Fe_3O_4 nanoparticles are grown on the surface of the GO sheets, the functional groups on the GO sheets act as templates, increasing crystallization and resulting in smaller sized Fe_3O_4 nanoparticles being resulted [7]. The peak positions of Fe_3O_4 nanoparticles are unchanged after encapsulation via polyaniline, which revealed that deposition of polyaniline on the surface of Fe_3O_4/GO has no influence on the crystallinity of Fe_3O_4/GO. The broadening of the diffraction peaks indicates nanoparticles nature of the sample. The crystallite size of sample, according to the FWHM of the (311) plane refraction peak, was estimated via the Debye-Scherrer formula through equation:

$$D = \frac{k\lambda}{\beta\cos\theta} \quad (1)$$

Where K is the shape factor, λ is the X-ray wavelength (0.154 nm), β is the full width at half maximum (FWHM) intensity of the peak, and θ is the Bragg angle [8]. D (in nm) is the average size of the ordered (crystalline) domains that may be smaller or equal to the grain size. The crystallite size thus obtained from this equation was found to be about 13 nm. However, no typical diffraction peaks of GO or polyaniline are observed in the prepared nanocomposite. This can be explained by the fact that only small amounts of GO and polyaniline are contained in the prepared nanocomposite [9].

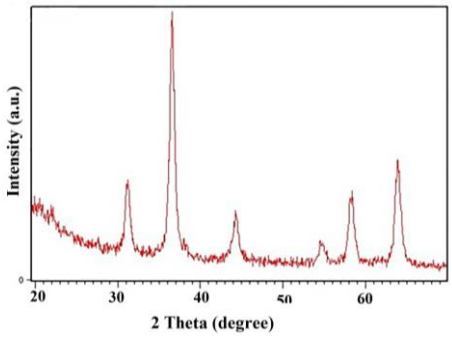

Fig. 1. XRD pattern of polyaniline- Fe_3O_4/GO nanocomposite.

3.1.2. SEM analysis of polyaniline- Fe_3O_4/GO *nanocomposite*

SEM image was recorded to understand the morphology and aggregation level of compounds. Fig. 2 shows SEM micrograph of polyaniline-Fe_3O_4/GO nanocomposite. The morphology of prepared nanocomposite seems to be sphere. Interestingly, the pure polyaniline agglomerates were not determined in SEM micrograph, which agrees with conclusions that polyaniline in polyaniline-Fe_3O_4/GO nanocomposite mainly covers the Fe_3O_4/GO surface [10]. As can be observed that, SEM image exhibits particles with good homogeneity, granular structure and slight agglomeration. Slight agglomeration can be because of the production of polyaniline on the surface of Fe_3O_4/GO nanoparticles which causes repulsion forces between nanoparticles and inhibits their agglomeration. Since less particle agglomeration occurred for polyaniline-Fe_3O_4/GO nanocomposite, the large surface area conveys high adsorption ability of this nanocomposite [11].

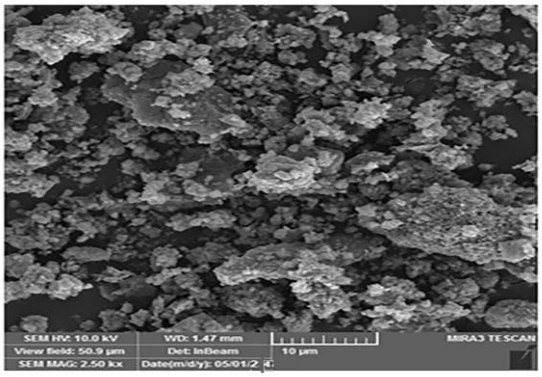

Fig. 2. SEM image of polyaniline- Fe_3O_4/GO nanocomposite**.**

3.1.3. Elemental analysis with EDX spectroscopy

The elemental composition of polyaniline-Fe_3O_4/GO nanocomposite was detected via EDX analysis. C, O, N and Fe peaks can be clearly observed from Fig. 3. EDX analysis demonstrated no significant levels of impurities, which could have originated from the process [12].

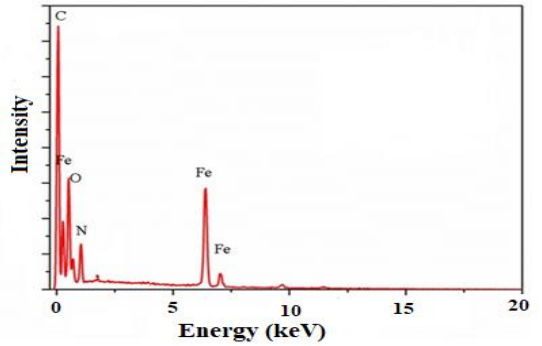

Fig. 3. EDX pattern of polyaniline- Fe_3O_4/GO nanocomposite.

3.1.4. FTIR spectrum of polyaniline-Fe_3O_4/GO *nanocomposite*

The FTIR spectrum of polyaniline-Fe_3O_4/GO nanocomposite is shown in Fig. 4. As can be seen, polyaniline shows the presence of the characteristic absorption bands at 1591 cm^{-1} (C=C stretching vibration of the quinoid ring), 1454 cm−1 (stretching vibration of C=C of the benzenoid ring), 1304 cm^{-1} (C–N stretching vibration), 1125 cm^{-1} (C–H in-plane deformation), and 811 cm^{-1} (C–H out of- plane deformation). The 788 and 580 cm^{-1} absorption peaks correspond to the Fe–O bond vibration of Fe_3O_4 nanoparticles [13]. The bands at 1605 and 1385 cm^{-1} are assigned to the characteristic peaks of C=O and C–O–C, respectively. The band at 2850 and 2920 cm^{-1} are assigned to the stretch vibration absorption of aliphatic C-H [14]. The adsorption peak at 3600 is due to the O–H stretching vibration [15]. Based on the above observation, we can find that the Fe_3O_4 nanoparticles, GO and polyaniline exist in the composite particles. It is known that graphene is an excellent electron acceptor, while, on the other hand, aniline is a very good electron donor [16]. As such, there is a donor–acceptor interaction, establishing the ground state charge-transfer complex between graphene and aniline. In this sense, the charge separated state of polyaniline takes the form of the positively charged emeraldine salt state, whereas GO becomes negatively charged and functions as an anionic counter ion to the emeraldine salt. Equilibrium between both species is established through charge transfer along the interface of polyaniline and graphene, resulting in partially charged species typical of charge-transfer complexes [17].

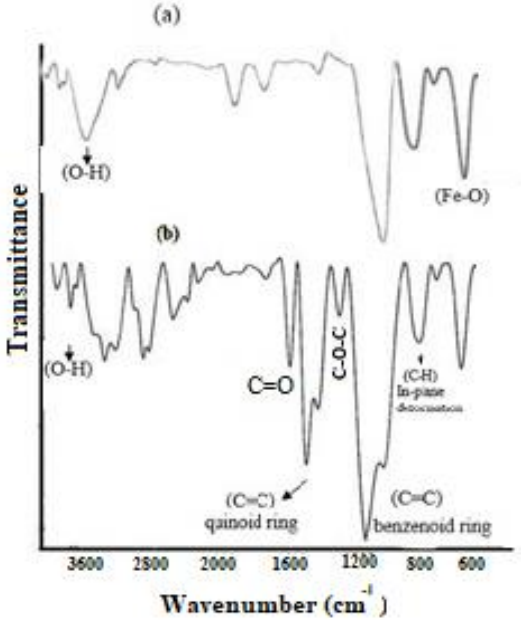

Fig. 4. FTIR spectra of (a) Fe_3O_4, (b) polyaniline-Fe_3O_4/GO samples.

DOI: 10.30473/IJAC.2024.72388.1307

3.2. Photocatalytic degradation of methyl red using prepared samples

Langmuir–Hinshelwood (L–H) kinetic model is the most commonly applied kinetic expression to explain the photocatalytic degradation of organic dyes from aqueous solutions [17]. The L–H kinetic equation is represented by Eq. 2:

$$\ln\frac{C_0}{C_t} = k_{obs}\, t \qquad (2)$$

where C_0 (mg L^{-1}) and C_t (mg L^{-1}) are the concentration of methyl red at 0 and t min, respectively. The apparent rate constant, k_{obs} (min^{-1}), is resulted from the slope of the $\ln\frac{C_0}{C_t}$ vs. time plot. The pseudo-first-order reaction rate constant (k_{obs}) can be selected as the basic kinetic parameter to compare the photocatalytic activity of prepared materials. The results of degradation of methyl red via prepared materials under black light irradiation are presented in Fig. 5. It could be observed that photocatalytic activity of Fe_3O_4/GO catalyst is higher than that of Fe_3O_4. It could be concluded that interactions between graphene and Fe_3O_4 lead to the improvement of the photocatalytic activity. It is known that Fe_3O_4 decorated on both sides of GO sheets may have increased their specific surface area, which resulted in enhanced degradation of dye molecules. Furthermore, the electrons on the graphene can be trapped by oxygen and water on the surface of Fe_3O_4/GO catalyst and produce the hydroxyl and superoxide radicals. As a result, electron–hole recombination is largely inhibited and this further facilitates the generation of more $OH^{\bullet}$ because of the valence band of Fe_3O_4 and the superoxide radical anions ($O_2^{\bullet-}$) at the surface of catalyst, which in turn results in a faster degradation of methyl red [18]. Also, the high photactivity can be attributed to the conductive bonding of Fe_3O_4 on the GO, which may lower the recombination of photocreated electron–gap pairs. This mechanism may be responsible for the increased removal efficiency of Fe_3O_4/GO compared to Fe_3O_4. During the photocatalytic process, methyl red was transformed into reactive, unstable intermediates and mineralized to colorless materials. Electron–hole pairs in the excited Fe_3O_4 could be efficiently detached to enable an effective change into photoinduced electrons from GO sheet to Fe_3O_4. This essential electron transfer mechanism can play a major role in the removal of pollutant [19]. As a result, the increased photocatalytic activity of Fe_3O_4/GO could play a critical role to solve pollutant related environmental problems.

From Fig. 5, photocatalytic activity of polyaniline-Fe_3O_4/GO is considerably higher than that of Fe_3O_4/GO. The photocatalytic degradation of methyl red can take place through a series of reactions on the surface of the materials, such as (i) interaction of methyl red with polyaniline-Fe_3O_4/GO nanocomposite, (ii) intermediate products (photocatalysis), (iii) colorless degradation product and (iv) saturation of polyaniline-Fe_3O_4/GO nanocomposite surface [34]. Polyaniline acts as a photosensitizer in polyaniline-Fe_3O_4/GO to sensitize the Fe_3O_4 surface. The conduction position of Fe_3O_4 was lower than the lowest unoccupied molecular orbital (LUMO) of polyaniline. The CB of Fe_3O_4 can act as a sink for photogenerated electrons in the hybrid photocatalyst. Under black-light irradiation, π–π transition occurred in polyaniline and electrons with highest occupied molecular orbital (HOMO) become excited and transfer to the LUMO of polyaniline. These electrons from the LUMO level are injected into the CB of Fe_3O_4, which react with molecular oxygen and generate $O_2^{\circ-}$ and $HO_2^{-\circ}$ in the aqueous solution [20]. Graphene nanosheets are well-known electron acceptor materials which used widely for decreasing the band gap of Fe_3O_4 to make it active in visible region via the energetically favored hybridization of C_{2p} and O_{2p} atoms of graphene and Fe_3O_4 [21]. So, the electrons from the CB of Fe_3O_4 and the LUMO of polyaniline may also be transferred to graphene. The electrons on the graphene can be trapped via oxygen and water on the surface of polyaniline-Fe_3O_4/GO and forme the hydroxyl and superoxide radicals. Furthermore, photogenerated holes in the HOMO level of polyaniline also generate hydroxyl radicals upon light excitation [22]. The following mechanism would be proffered for the photocatalytic reactions.

Polyaniline + hύ → ⟦Polyaniline (h⟧^(+) + e^(-)) (3)

⟦Polyaniline (h⟧^(+)) + H_2O → Polyaniline + H^(+) + ⟦OH⟧^(.) (4)

⟦Polyaniline (h⟧^(+)) + ⟦OH⟧^(-) → Polyaniline + ⟦OH⟧^(.) (5)

⟦Polyaniline (e^(-)⟧^) + Graphene → Polyaniline + Graphene (e^(-)) (6)

⟦Polyaniline (e^(-)⟧^)+ Fe_3O_4 → Polyaniline + Fe_3O_4 (e^(-)) (7)

⟦Graphene (e⟧^(-)) + O_2 → Graphene + O_2^(.) (8)

Fe3O4 (e^(-)) + O_2 → Fe_3O_4 + O_2^(.-) (9)

O_2^(.-) + H2O → ⟦OH⟧^(.) (10)

⟦OH⟧^(.) + pollutant → CO_2 + H_2O (11)

Furthermore, in polyaniline-Fe_3O_4/GO samples, the polyaniline content can play a significant role in affecting photocatalytic activity of photocatalysts. The results of degradation of methyl red by polyaniline-Fe_3O_4/GO catalysts with various polyaniline contents (4 polyaniline-Fe_3O_4/GO, 8 polyaniline-Fe_3O_4/GO, 12 polyaniline-Fe_3O_4/GO, 16 polyaniline- Fe_3O_4/GO

DOI: 10.30473/IJAC.2024.72388.1307

and 20 polyaniline-Fe_3O_4/GO) are shown in Fig. 5. From 4 polyaniline- Fe_3O_4/GO to 12 polyaniline-Fe_3O_4/ GO, the photocatalytic activity was gradually enhanced, and 12 polyaniline- Fe_3O_4/GO showed the maximized catalytic activity. Based on results, when the content of polyaniline is more increased above its optimum value, the photocatalytic performance deteriorated. The high photoactivity of 12 polyaniline-Fe_3O_4/GO can be explained as following reasons:

• The presence of imperfections may omit the polyaniline chain stretching process [35], which decline polyaniline conductivity.

• Because of high aniline concentrations, oxidation products with amino groups in the ortho-position (i.e., imperfections) can be produced, which may alert the polyaniline chain structure and consequently polymer-pollutant interactions [23].

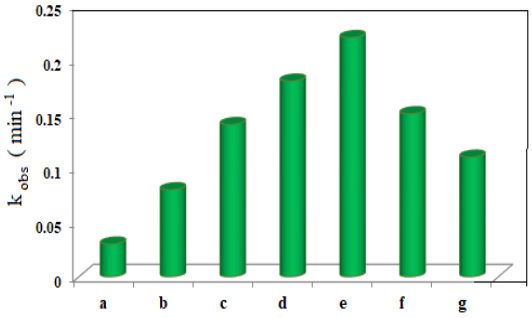

Fig. 5. Photocatalytic degradation of methyl red in the presence of (a) Fe_3O_4, (b) Fe_3O_4/GO, (c) 4 polyaniline- Fe_3O_4/ GO, (d) 8 polyaniline-Fe_3O_4/GO, (e) 12 polyaniline- Fe_3O_4/GO, (f) 16 polyaniline- Fe_3O_4/GO and (g) 20 polyaniline-Fe_3O_4/GO.

3.3. Adsorptive degradation of *methyl red by prepared samples*

Fig. 6 shows the adsorptive removal of methyl red from aqueous solution via polyaniline-Fe_3O_4/GO and Fe_3O_4/GO samples. Results showed that efficiency of methyl red degradation in the presence of polyaniline-Fe_3O_4/GO is higher. Accumulation of a substance between the liquid–solid interface or gas–solid interface due to physical or chemical associations is termed an adsorption process. Adsorption procedure is controlled by physical factors on most of the adsorbents such as polarity, Van der Waals forces, hydrogen bonding, dipole–dipole interaction, π–π interaction, etc. [24]. So, the design of an adsorbent generally depends on the type of substance to be adsorbed or removed. Methyl red is an anionic dye that can be degraded by an adsorbent showing strong affinity toward negatively-charged species. Polyaniline in its conductive emeraldine salt state possesses a large number of amine (–N<) and imine (–N=) functional groups and substantial amounts of positive charges localized over its backbone, making it an efficient candidate for the adsorption of negatively polarized materials. This electrostatic force of attraction could be the essential driving force leading to the increased adsorption of methyl orange. So, the presence of polyaniline in synthesized nanocomposite plays a crucial role in the removal of anionic dye from arouse solutions [23].

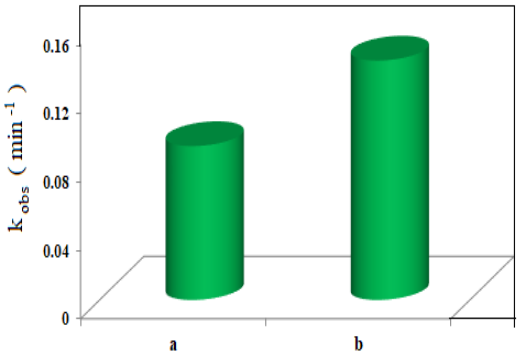

Fig. 6. Adsorptive removal of methyl red from aqueous solution in the presence of (a) Fe_3O_4/GO and (b) polyaniline- Fe_3O_4/ GO samples.

3.4. Adsorption isotherm studies

In order to evaluate the nature of adsorption procedure, the equilibrium adsorption isotherms were studied. Adsorption isotherms are applied to explain the interaction of solutes with adsorbent. Equilibrium adsorption isotherm data were analyzed according to the linear forms of Langmuir and Freundlich adsorption isotherm equations (12–13), respectively [25]:

$$\frac{1}{q_e} = \left(\frac{1}{K_l q_m}\right)\frac{1}{C_e} + \frac{1}{q_m} \qquad (12)$$

$$\ln q_e = \frac{1}{n} ln C_e + ln K_F \qquad (13)$$

where C_e (mg L^{-1}) is the equilibrium concentration of methyl red, q_e (mg g^{-1}) is the content of methyl red adsorbed at equilibrium, q_m (mg g^{-1}) is the maximum adsorption at monolayer and K_L (L mg^{-1}) is the Langmuir constant including the affinity of binding sites. K_F [(mg g^{-1}) (L $mg^{-1})^{1/n}$] and n are the Freundlich constants implying adsorption capacity and intensity, respectively. The values of Langmuir and Freundlich parameters were estimated from the slope and intercept of linear plots of $1/q_e$ versus $1/C_e$ and ln q_e versus ln C_e, respectively. Fig. 7 displays the adsorption isotherms plots. From the slopes and intercepts, the values of q_m, K_L, n and K_F, were calculated and represented in Table 1. It can be observed from Table 1 that the adsorption process could be described via all models from comparing the results of the correlation coefficient values. However, careful observation may explain

DOI: 10.30473/IJAC.2024.72388.1307

Langmuir isotherm better than others. As can be observed in Table 1, the obtained correlation coefficient for Langmuir isotherm model was higher than that of other model, which implies the suitability of Langmuir isotherm model for describing adsorption of methyl red onto polyaniline-Fe_3O_4/GO nanocomposite. Based on Langmuir model, the maximum adsorption capacity of polyaniline-Fe_3O_4/GO nanocomposite for the adsorption of methyl red was found to be 101.72 mg g^{-1}. Essential features of Langmuir isotherm model can be represented in term of separation factor, R_L, as below equation:

$$R_L = \frac{1}{1 + K_l C_0} \qquad (14)$$

where C_o (mg L^{-1}) is the initial pollutant concentration [24].

The values of R_L arranged as $R_L = 0$, $0 < R_L < 1$ and $R_L > 1$ indicate that adsorption is irreversible, favorable and unfavorable, respectively. Table 1 demonstrates that R_L values are between 0.27 and 0.84, which implies the adsorption of methyl red onto polyaniline-Fe_3O_4/GO nanocomposite is favorable [25].

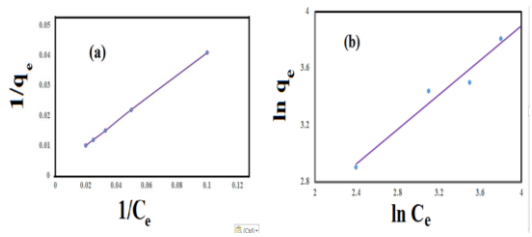

Fig. 7. Plots of linearized Langmuir (a) and Freundlich (b) adsorption isotherms for methyl red adsorption onto polyaniline- Fe_3O_4/ GO nanocomposite.

[Table 1] Isotherm parameters for methyl red adsorption onto polyaniline- Fe_3O_4/ GO nanocomposite.

Type of isotherm model	Value
Langmuir isotherm	
q_m (mg g^{-1})	101.72
K_L (L mg^{-1})	0. 183
R_L	0.27-0.84
R^2	0.9998
Freundlich isotherm	
K_F (mg g^{-1})	3.72
n	1.58
R^2	0.9677

3.5. Comparison of photodegradation and adsorption of methyl red using polyaniline-Fe_3O_4/ GO nanocomposite

The removal rate of methyl red by photolysis and adsorption processes in the presence of polyaniline-Fe_3O_4/GO nanocomposite is depicted in Fig 8.

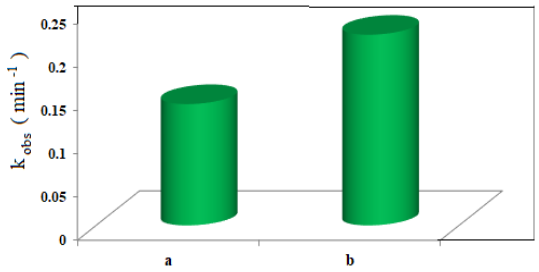

Fig. 8. Degradation rates of methyl red in the presence of polyaniline-Fe_3O_4/GO nanocomposite under (a) Adsorption process and (b) UV-visible radiation.

It can be observed that the removal rate of methyl red by polyaniline- Fe_3O_4/GO nanocomposite under photocatalytic process was considerably higher than the adsorption process, indicating that the synergistic adsorption-photocatalysis had definitely occurred. It can be concluded that during the removal of methyl red using polyaniline-Fe_3O_4/GO nanocomposite under light irradiation, both adsorption and photocatalytic processes occurred simultaneously. During the experiment in the dark, the rate of removal of methyl red by the adsorption process was calculated to be 0.16 min^{-1}. However, when polyaniline-Fe_3O_4/GO nanocomposite was exposed to light irradiation, the rate of removal of methyl red jumped to 0.25 min^{-1} implying that both photocatalytic and adsorption processes manifested simultaneously.

Fig. 9 demonstrates the UV-vis spectral changes of methyl red aqueous solution in the procedure of photodegradation by polyaniline- Fe_3O_4/ GO. From this figure, it is observed that, the absorbance at 520 nm of methyl red decreases gradually with time elapsed: which implies the reduction of methyl red from red to colorless. The absorption peak completely disappeared in 28 min which confirms the complete degradation of methyl red.

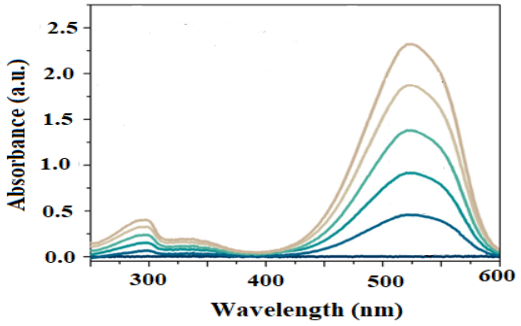

Fig. 9. UV-vis spectral changes of methyl red during degradation procedure as a function of reaction time using polyaniline-Fe_3O_4/Graphene oxide nanocomposite.

DOI: 10.30473/IJAC.2024.72388.1307

4. CONCLUSIONS

The present study was carried out to prepare and investigate the efficiency of polyaniline-Fe_3O_4/GO nanocomposite to adsorb and degrade an anionic dye (methyl red) from aqueous solution. The results showed that polyaniline-Fe_3O_4/GO nanocomposite is more effective in the comparison with Fe_3O_4, and Fe_3O_4/GO catalysts. SEM analysis proved a highly porous structure for polyaniline-Fe_3O_4/GO nanocomposite, which is suitable for sequestering pollutant molecules in aqueous solutions. Based on results, in polyaniline-Fe_3O_4/GO samples, the polyaniline value may play an important role in affecting photocatalytic activity of photocatalysts. When the content of polyaniline is more increased above its optimum content, the photocatalytic performance decreased. Among various isotherm models, the Langmuir isotherm implied the best fit to experimental data. The maximum methyl red adsorption capacity was predicted as 101.72 mg g^{-1} via Langmuir model. The obtained value for separation parameter pertaining to Langmuir model implied favorable adsorption of methyl red onto polyaniline-Fe_3O_4/GO nanocomposite. The separation factor, R_L, was obtained less than 1, indicating the favorable nature of methyl red adsorption on polyaniline-Fe_3O_4/GO nanocomposite.

Acknowledgment

The author acknowledges the support of Payame Noor University of Iran.

REFERENCES

[1] S. Abdalkareem Jasima, M. M. Kadhim, B. Abed Hussein, S. Emad Izzate, and Z. Mohsen Najmf, Photocatalytic Degradation of Rhodamine B and Methylene blue Using α-Fe2O3 Nanoparticles, *Phys. Chem. Res*., 11 (2023) 139-147.

[2]E. Parthiban, N. Kalaivasan, and S. Sudarsan, A study of magnetic, antibacterial and antifungal behaviour of a novel gold anchor of polyaniline/ itaconic acid/Fe3O4 hybrid nanocomposite: Synthesis and characterization, *Arabian. J. Chem*., 13 (2020) 4751–4763.

[3]Z. Dong, Q. Zhang, B. Y. Chen, and J. Hong, Oxidation of bisphenol A by persulfate via Fe3O4- α-MnO2 nanoflflower-like catalyst: Mechanism and efficiency, Chem. Eng. J., 357 (2019) 337–347.

[4]R. Nawaz, S. Zulfqar, M. I. Sarwar, and M. Iqbal, Synthesis of diglycolic acid functionalized coreshell silica coated Fe3O4 nanomaterials for magnetic extraction of Pb(II) and Cr(VI) ions, *Sci. Rep*., 10 (2020) 1–13.

[5] H. J. Seo, J. W. Lee, Y. Hoon Na, and Jin. H. Boo, Enhancement of Photocatalytic Activities with Nanosized Polystyrene Spheres Patterned Titanium Dioxide Films for Water Purification, *Catalysts*, 10 (2020) 886-898.

[6]R. Mohammadi, and M. Alizadehlarijan, Proficient Adsorption, Photodegradation and Sonodegradation of Methylene Blue by Fe3O4/Graphene Nanocomposite, *Iran. J. Anal. Chem.*, 10 (2023) 61-71.

[7]M. Na. Pervez, W. He, T. Zarra, V. Naddeo, and Y. Zhao, New Sustainable Approach for the Production of Fe3O4/Graphene Oxide-Activated Persulfate System for Dye Removal in Real Wastewater, *Water*., 12 (2020) 733-749.

[8] R. Mohammadi, Highly Efficient catalyst of TiO2/chitosan for Photodegradation and Sonodegradation of Organic Pollutants, *Chem. Rev. Lett*., 5 (2023) 133-140.

[9]M. Maruthupandy, T. Muneeswaran, M. Anand, and F. Quero, Highly effificient multifunctional graphene/chitosan/magnetite nanocomposites for photocatalytic degradation of important dye molecules, *Int. J. Bio. Macromol*, 153 (2020) 736–746.

[10]. Sarkar, N. T. Ponce, A. Banerjee, R. Bandopadhyay, S. Rajendran, E. Lichtfouse photocatalytic degradation of dyes: a review, *Environ. Chem. Lett*., 18 (2020) 1569–1580.

[11]V.K. Nathan, P. Ammini, and J. Vijayan, Photocatalytic degradation of synthetic dyes using iron (III) oxide nanoparticles (Fe2O3 Nps) synthesized using Rhizophora mucronata Lam, *IET Nanobiotechnol*., 13 (2019) 120-123.

[12]A.M. Tayler, R. Farouq, O.A. Mohamed, M.A. Tony, Oil spill clean-up usingcombined sorbents: A comparative investigation and design aspects, *Int. J. Environ. Anal. Chem*., 100 (2020) 311–323.

[13]M. Liu, Y. Liu, Y. Ge, Z. Zhong, Z. Wang, T. Wu, X. Zhao, and Y. Zu, Solubility, Antioxidation, and Oral Bioavailability Improvement of Mangiferin Microparticles Prepared Using the Supercritical Antisolvent Method, *Pharmaceutics*., 12 (2020) 90-104.

[14]A. Rawat, W. Baille, and S. Tripathy, Swelling behavior of compacted bentonite-sand mixture during water infiltration, *Eng. Geol.*, 257 (2019) 105141.

[15]A.H. Elgarhy, B.N. A. Mahran, G. Liu, T. A. Salem, E.S. ElBastamy ElSayed, and L. A. Ibrahim, Comparative study for removal of phosphorus from aqueous solution by natural and activated bentonite, *Sci. Rep*., 12 (2022) 19433.

[16]R. Mohammadi, B. Massoumi, and A. Mashayekhi, Comparative Study on Ability of Some Magnetic Nanocompounds of Fe3O4, Fe3O4/Polystyrene and Fe3O4/Polyaniline to Remove of Methyl Orange from Aqueous Solutions, *Iran. J. Anal. Chem*., 10 (2023) 22-29.

[17]Y. Wu, S. Zeng, F. Wang, M. Megharaj, R. Naidu, and Z. Chen, Heterogeneous Fenton-like oxidation of malachite green by iron-based nanoparticles synthesized by tea extract as a catalyst, *Sep Purif. Technol*., 154 (2015) 161-167.

[18]B. Sarwan, B. Pare, and A.D. Acharya, Heterogeneous photocatalytic degradation of Nile blue dye in aqueous BiOCl suspensions, *Appl. Surf. Sci*., 301 (2014) 99-106.

[19] H. Wu, X. Dou, D. Deng, Y. Guan, L. Zhang, and G. He, Decolourization of the azo dye Orange G in aqueous solution via a heterogeneous Fenton-like reaction catalyzed by goethite. *Environ Techno*. 33 (2012) 1545-1552.

[20]R. Mohammadi, B. Massoumi, and R. Mashayekhi, Fe3O4/polystyrene-alginate as a novel adsorbent for highly efficient removal of dyes, *J. Chem. Chem. Eng*., 41 (2022) 3553-3566.

[21]E. Ghoohestani, F. Samari1, A. Homaei, and S. Yosuefnejad, A facile strategy for preparation of Fe3O4 magnetic nanoparticles using Cordia myxa leaf extract and investigating its adsorption activity in dye removal, *Scie. Reports*, 14 (2024) 84.

[22] C. Prasad, G. Yuvaraja, and P. Venkateswarlu, Biogenic synthesis of Fe3O4 magnetic nanoparticles using Pisum sativum peels extract and its efect on magnetic and Methyl orange dye degradation studies. *J. Magn. Magn. Mater*., 424 (2017) 376–381.

[23]N. Sebeia, M. Jabli, and A. Ghith, Biological synthesis of copper nanoparticles, using Nerium oleander leaves extract: Characterization and study of their interaction with organic dyes, *Inorg. Chem. Commun*., 105 (2019) 36–46.

[24]C. J. Pandian, R. Palanivel, and S. Dhananasekaran, Green synthesis of nickel nanoparticles using Ocimum sanctum and their application in dye and pollutant adsorption. *Chin. J. Chem. Eng*., 23 (2015) 1307–1315.

[25]R. Mohammadi, B. Massoumi, and F. Galandar, Polyaniline-TiO2/graphene:an efficient catalyst for the removal of anionic dyes, *Desal. Wat. Treat*, 142 (2019) 321–330.

DOI: 10.30473/IJAC.2024.72388.1307

بررسی تاثیر مقدار پلی آنیلین در فعالیت کاتالیزوری نانوکامپوزیت Fe_3O_4/GO

رباب محمدی
بخش شیمی، دانشگاه پیام نور، تهران، ایران
* E-mail: rb_mohammadi@pnu.ac.ir; mohammadi_rb@yahoo.com
تاریخ دریافت: ۱۸ خرداد ۱۴۰۳ **تاریخ پذیرش:** ۱۴ شهریور ۱۴۰۳

چکیده

در این تحقیق Fe_3O_4, Fe_3O_4/graphene oxide (Fe_3O_4/GO) و polyaniline-Fe_3O_4/GO با مقادیر مختلفی از پلی آنیلین تهیه و با روشهای آنالیزی مختلف نظیر XRD, SEM, EDX و FT-IR مقایسه شدند. از نمونه های تهیه شده برای حذف متیل رد به عنوان رنگ آنیونی از محلول های آبی استفاده شد. نانوکامپوزیت polyaniline-Fe_3O_4/GO فعالیت کاتالیزوری بالاتری نشان داد که تا حدودی به دلیل اثر حساس کنندگی پلی آنیلین و سرعت پایین ترکیب مجدد حفره- الکترون به دلیل خاصیت الکترون کشندگی اکسید گرافن است. واکنش تخریب نوری با مدل لانگمویر تطابق خوبی نشان داد که بیانگر وابستگی سرعت واکنش به مرحله جذب سطحی است. همچنین در نانوکامپوزیت polyaniline-Fe_3O_4/GO مقدار پلی آنیلین نقش تعیین کننده ای در فعالیت فتوکاتالیزوری نمونه ها ایفا می کند. بر اساس نتایج به دست آمده وقتی مقدار پلی آنیلین از میزان بهینه بالاتر می رود فعالیت کاتالیزوری کاهش می یابد. همچنین کارایی نانوکامپوزیت polyaniline-Fe_3O_4/GO به منظورحذف متیل رد از طریق فرایندهای فتو کاتالیزوری و جذب سطحی مورد مقایسه قرار گرفت. بر اساس نتایج به دست آمده سرعت حذف متیل رد از طریق فرایندهای فتو کاتالیزوری بیشتر است. برای تشخیص نوع ایزوترم جذب، ایزوترم های جذب لانگمویر و فروندلیچ مورد مطالعه قرار گرفتند. مدل لانگمویر با داده های آزمایشگاهی تطابق خوبی نشان داد. با توجه به مدل لانگمویر، polyaniline-Fe_3O_4/GO بالاترین ظرفیت جذب متیل رد را با ۱۰۱,۷۲ میلی گرم در گرم نشان داد.

کلید واژه ها

نانوکامپوزیت polyaniline-Fe3O4/GO؛ متیل رد؛ فعالیت فتو کاتالیزوری؛ فرایند جذب سطحی.

DOI: 10.30473/IJAC.2024.72388.1307